

Experimental and Computational Evidence of the Biradical Structure and Reactivity of Titanium(IV) Enolates

Carlos Heras, Alejandro Gómez-Palomino, Pedro Romea, Félix Urpí, Josep Maria Bofill, and Ibério de P.R. Moreira

J. Org. Chem., **Just Accepted Manuscript** • DOI: 10.1021/acs.joc.7b01174 • Publication Date (Web): 07 Aug 2017

Downloaded from <http://pubs.acs.org> on August 15, 2017

Just Accepted

“Just Accepted” manuscripts have been peer-reviewed and accepted for publication. They are posted online prior to technical editing, formatting for publication and author proofing. The American Chemical Society provides “Just Accepted” as a free service to the research community to expedite the dissemination of scientific material as soon as possible after acceptance. “Just Accepted” manuscripts appear in full in PDF format accompanied by an HTML abstract. “Just Accepted” manuscripts have been fully peer reviewed, but should not be considered the official version of record. They are accessible to all readers and citable by the Digital Object Identifier (DOI®). “Just Accepted” is an optional service offered to authors. Therefore, the “Just Accepted” Web site may not include all articles that will be published in the journal. After a manuscript is technically edited and formatted, it will be removed from the “Just Accepted” Web site and published as an ASAP article. Note that technical editing may introduce minor changes to the manuscript text and/or graphics which could affect content, and all legal disclaimers and ethical guidelines that apply to the journal pertain. ACS cannot be held responsible for errors or consequences arising from the use of information contained in these “Just Accepted” manuscripts.



Experimental and Computational Evidence of the Biradical Structure and Reactivity of Titanium(IV) Enolates

Carlos Heras,[†] Alejandro Gómez-Palomino,^{†, ‡} Pedro Romea,^{*, †, ‡} Fèlix Urpí,^{*, †, ‡}

Josep Maria Bofill,^{*, †, §} and Ibério de P. R. Moreira^{*, # §}

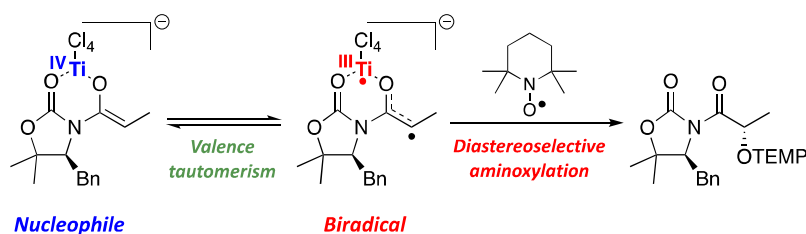
[†] *Departament de Química Inorgànica i Orgànica, Secció de Química Orgànica, Universitat de Barcelona, Carrer Martí i Franqués 1-11, 08028 Barcelona, Catalonia, Spain.*

[‡] *Institut de Biomedicina (IBUB), Universitat de Barcelona.*

[§] *Institut de Química Teòrica i Computacional de la Universitat de Barcelona (IQTCUB)*

[#] *Departament de Ciència dels Materials i Química Física, Secció de Química Física, Universitat de Barcelona Carrer Martí i Franqués 1-11, 08028 Barcelona, Catalonia, Spain*

E-mail: i.moreira@ub.edu



Abstract: Quantum chemical calculations have unveiled the unexpected biradical character of titanium(IV) enolates from *N*-acyl oxazolidinones and thiazolidinethiones. The electronic structure of these species therefore involves a valence tautomerism consisting of an equilibrium between a closed shell (formally Ti(IV) enolates) and an open shell, biradical, singlet (formally Ti(III) enolates) electronic states, whose origin is to be basically found in changes of the Ti–O distance. Spectroscopic studies of the intermediate species lend support to such a model, which also turns out to be crucial for a better understanding of the overall reactivity of titanium(IV) enolates. In this context, a thorough computational analysis of the

1
2
3 radical addition of titanium(IV) enolates from *N*-acyl oxazolidinones to TEMPO has
4
5 permitted us to suggest an entire mechanism, which accounts for the experimental details and
6
7 the diastereoselectivity of the process. All together, this evidence highlights the relevance of
8
9 biradical intermediates from titanium(IV) enolates and may be a useful contribution to the
10
11 foundations of a more insightful comprehension of the structure and reactivity of titanium(IV)
12
13 enolates.
14
15
16
17
18
19

20 INTRODUCTION

21
22
23 Metal enolates play a crucial role in a wide range of carbon–carbon as well as carbon–
24
25 heteroatom bond forming reactions and are therefore among the most important nucleophilic
26
27 species in organic synthesis.^{1–3} Alkylation or aldol reactions are well-known examples of the
28
29 sort of transformations that hinge on the enolization of a parent carbonyl compound and the
30
31 reactivity of the resultant enolate.^{3–5} Therefore, great effort has been dedicated to the
32
33 development of increasingly more efficient enolization procedures that supply metal enolates
34
35 capable of participating in highly selective reactions.⁶ As a result of such research, a handful
36
37 of procedures have emerged as the most appropriate to obtain metal enolates with remarkable
38
39 regio- and stereocontrol, which can subsequently react with a broad range of electrophiles
40
41 under a variety of mild conditions.⁷ A proper understanding of these processes is thus
42
43 fundamental to appreciate the prominent role of metal enolates as nucleophilic reagents in
44
45 organic transformations that are governed by heterolytic mechanisms.
46
47
48

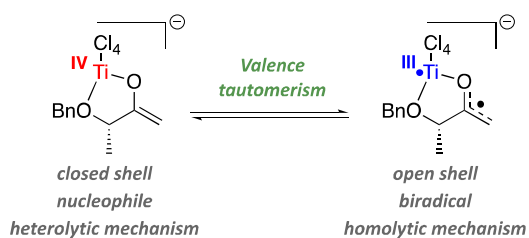
49
50 In such a scenario, the metal counterpart is only required to provide oxygen-bound metal
51
52 enolates with a defined geometry that interact with electrophiles through tight and ordered
53
54 transition states. Therefore, the importance of the metal depends on its influence on both the
55
56 structure and the reactivity of the *organic* part of the enolate. The alternative point of view
57
58
59
60

1
2
3 concerning the inverse effect of the *organic* part of the enolate on the *metal* has hardly been
4
5 considered. Nevertheless, such a perspective could reveal new forms of reactivity that are
6
7 complementary to the aforementioned nucleophilic pathway.
8

9
10 The *non-innocent ligand* concept, expounded by Jørgensen in the 1960s,⁸ can be useful to
11
12 address such a shift in the reacting paradigm. The concept applies to those ligands that can
13
14 alter the oxidation state of the metal, which dramatically affects the reactivity of the overall
15
16 organometallic species.^{9,10} Unfortunately, the theoretical background for such a phenomenon
17
18 is often misunderstood since it can imply either a resonance case for a single minimum or a
19
20 real equilibrium between two different species in a double minimum arrangement. The former
21
22 corresponds to a *hybrid valence bond* electronic state of a given molecular structure, while the
23
24 latter properly corresponds to a *valence tautomer*.¹¹ Irrespective of the theoretical model that
25
26 best fits this situation, the main consequence of this new approach is that the metal and the
27
28 ligand can act in a synergistic manner thereby enabling new chemical transformations to
29
30 occur.
31
32

33
34 Within this framework, some years ago we reported the unexpected biradical character of
35
36 titanium(IV) enolates derived from α -benzyloxy ketones¹² and TiCl₄-phenoxy complexes¹³
37
38 that were assigned to coexisting Ti(III) species. Rather than being a simple expansion of the
39
40 resonance model, this biradical character arises from a valence tautomerism in which there is a
41
42 nuclear configuration with two utterly unlike but almost degenerate electronic configurations.
43
44 Indeed, the very nature of these electronic configurations is, to a large extent, distinct: one
45
46 corresponds to a closed shell electronic state, whereas the other has a marked open shell,
47
48 delocalized *biradical*, character, which requires an electron transfer from the organic ligand to
49
50 the titanium metal. Therefore, the closed shell electronic configuration would be responsible
51
52 for the classical nucleophilic reactivity observed for these titanium(IV) enolates¹⁴ whereas the
53
54 open shell might be the origin of the aforementioned *biradical* character and the basis for a
55
56
57
58
59
60

new reacting paradigm: titanium(IV) enolates can also participate in homolytic or radical additions (Scheme 1).



Scheme 1. Valence tautomerism in titanium(IV) enolates¹²

Hence, the reactivity of titanium(IV) enolates would follow different lines if their *organic* part acted as a non-innocent ligand and thus affected the oxidation state of the metal. The interaction of such a ligand with the metal might dramatically change the electronic distribution of the ligand itself and activate new and unexpected reactivity of it. Homocoupling of certain enolates derived from phenylacetic derivatives^{15,16} and other occasional pieces of evidence in the literature¹⁷ had already suggested the feasibility of such a new reaction mode. Interestingly, Zakarian recently proved that titanium(IV) enolates derived from chiral *N*-acyl oxazolidinones could indeed react stereoselectively with carbon- as well as oxygen-based radicals through a homolytic mechanism (Equation 1 and 2 in Scheme 2).^{18–20}

1
2
3 nucleophilic titanium(IV) enolates are associated with biradical Ti(III) species through a
4
5 valence tautomery equilibrium, which basically hinges on differences of Ti–O bond distance
6
7 in the case of oxazolidinones, and a more complex distortion of the Ti–S bond in the case of
8
9 thiazolidinethiones. Further studies have also revealed that a radical-like mechanism
10
11 successfully accounts for the reaction of titanium(IV) enolates from **1** with TEMPO.
12
13 Importantly, these calculations account for the diastereoselectivity observed in the
14
15 aminoxylation reactions shown in Scheme 2. All together, these results strongly support the
16
17 new reacting paradigm of titanium(IV) enolates.
18
19
20
21
22
23
24
25
26
27
28
29
30
31
32
33
34
35
36
37
38
39
40
41
42
43
44
45
46
47
48
49
50
51
52
53
54
55
56
57
58
59
60

RESULTS AND DISCUSSION

Analysis of the valence tautomerism in the titanium(IV) enolates

With the aim of providing a theoretical account of the valence tautomerism associated with the titanium(IV) enolates described in Scheme 2, we initially studied the electronic and molecular structures of simple chiral models **1** and **2** in detail (Figure 1).

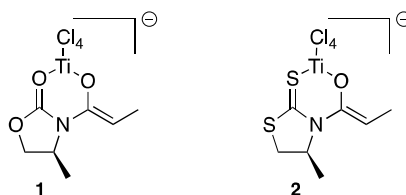


Figure 1. Models used to investigate the *valence tautomerism* of the titanium(IV) enolates reported in this work.

The molecular structure of titanium enolate **1** features an almost planar chelate with four chlorine atoms directly bound to the hexacoordinated titanium, which can be properly described by means of a closed shell electronic configuration. Nevertheless, a high polarization of the electron density of the TiCl_4 moiety towards the chlorine atoms and the availability of empty d-orbitals for the metal facilitated open shell configurations. Indeed, our calculations identified low energy open shell singlet (OSS) and triplet (T) electronic states with a very strong biradical character in which one electron is mainly located over the titanium atom and the other one forms an allylic-like system $[\text{O}-\text{CR}-\text{CH}_2]^\bullet$. Such a species might be classified as a titanium(III) enolate. Our results indicate that this is close in energy to the titanium(IV) enolate, and these two species are connected through a reaction path with a low energy barrier. Analysis of Ti–O bonds both in closed- and open-shell configurations also

suggests that these interactions are dative in nature. The most relevant valence (natural) orbitals of this biradical, along with the corresponding occupation numbers are shown in Figure 2.

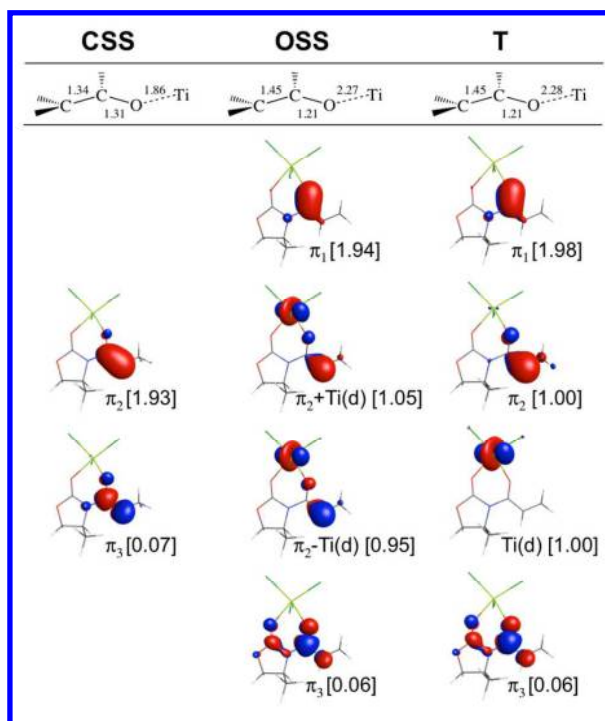


Figure 2. Relevant CASSCF(8,7) natural orbitals of the electronic configurations of **1** and selected distances of optimized structures. Values in square brackets are the corresponding occupation numbers.

The topology of these orbitals allows us to assign these orbitals to an allylic-like π -system (π_1 , π_2 , and π_3 orbitals) combined with the Ti d orbital, Ti(d). Orbitals π_1 and π_3 involve the bonding and antibonding combinations of the allyl-like π -system. In turn, the non-bonding π_2 and Ti(d) orbitals can mix to produce orbitals $\pi_2 + \text{Ti}(d)$ and $\pi_2 - \text{Ti}(d)$ with occupations close to unity. These account for the biradical character. In addition, the positive overlap between π_2 and Ti(d) increases as the Ti–O distance diminishes when the biradical evolves towards the closed shell configuration through an intersystem crossing as expected for a valence

tautomerism process.¹² We can understand both the structure and the reacting pattern of such species by means of the electronic profiles model proposed by Salem.²³ It includes the three curves represented in Figure 3 to describe the main electronic configurations defining the lowest energy electronic states involved in the valence tautomerism: one curve describes the closed shell configuration (Ψ_{cs}) whereas the two other curves describe the open shell or biradical configurations (Ψ_{os}^{sing} , Ψ_{os}^{trip}), which are all low-lying electronic states of the system with very similar molecular geometries.

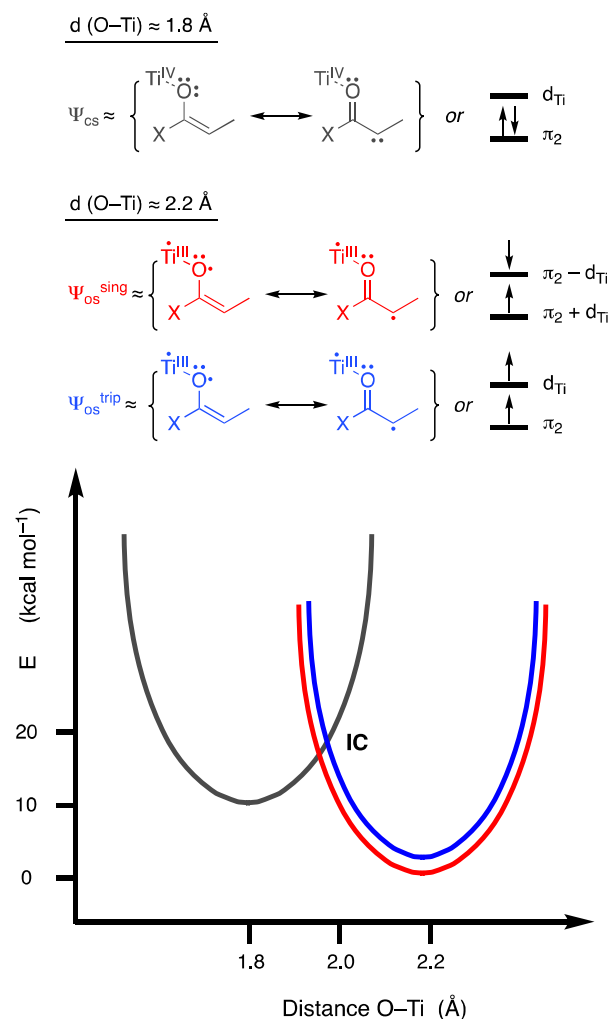


Figure 3. Description of the electronic states involved in the valence tautomerism.

1
2
3 The energies of the triplet and singlet biradical states, $\Psi_{\text{os}}^{\text{trip}}$ and $\Psi_{\text{os}}^{\text{sing}}$ respectively, are very
4 similar and the states are found to have almost identical geometric and electronic features as
5 can be deduced from the topology of their most significant orbitals shown in Figure 2. In turn,
6 the intersection of the Ψ_{cs} with the $\Psi_{\text{os}}^{\text{sing}}$ and $\Psi_{\text{os}}^{\text{trip}}$ curves corresponds to an intersystem
7 crossing (IC in Figure 3). In particular, the crossing of Ψ_{cs} with $\Psi_{\text{os}}^{\text{sing}}$ corresponds to a
8 *seam*,²⁴ and determines the barrier for the interconversion closed shell/biradical species.
9 Noticeably, this valence bond representation of the electronic states is valid in the regions
10 near the corresponding minima and far from the intersection of states where quasidegeneracy
11 induces a strong mixing of electronic states (Figure 3).
12
13
14
15
16
17
18
19
20
21
22

23 The minimum energy structure corresponds to the OSS electronic state for **1** because the
24 unfavourable electronic repulsion is compensated by the charge interaction with the titanium
25 atom. In turn, the single occupied orbitals of the biradical structures correspond to a more
26 stable electronic structure than a hypothetical closed shell, because the unfavourable electron–
27 repulsion of the two electrons is not compensated by the titanium charge. The metal is too far
28 from the C–C–O moiety with respect to the closed shell and this is the reason why the
29 unfavourable repulsion is compensated by shortening the Ti–O distance. Indeed, the dual
30 electronic structure obtained by a small change in the Ti–O distance characterizes the valence
31 tautomerism of the titanium(IV) enolates.
32
33
34
35
36
37
38
39
40
41
42

43 Comprehensive analysis of such configurations of **1** revealed that their geometrical
44 differences do not exceed 0.5 Å, at the most (see Figure 2). Nevertheless, the most stable
45 geometry of the CSS configuration features a short Ti–O distance, without single and double
46 bond alternation. Instead, the O–C distance becomes shorter and the C–C distance longer in
47 the minimum energy structure for both the T and the OSS radical configurations, which
48 display bond alternation. Most importantly, the energy gap between the closed and open shell
49 configurations decreases as the Ti–O distance increases and at ≈ 1.9 Å the biradical
50
51
52
53
54
55
56
57
58
59
60

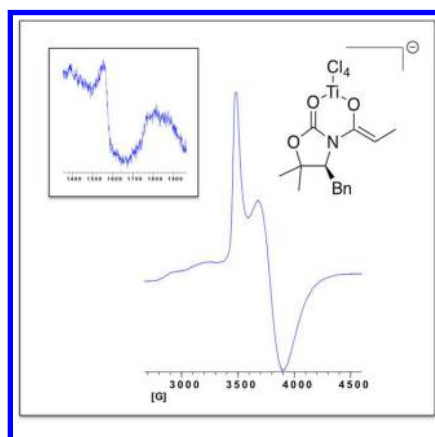
1
2
3 configurations become more stable than the closed configuration. However, it was not
4 possible to locate the stationary point due to the planarity of the potential energy surface
5 (PES) in this region and the fact that the Born-Oppenheimer approximation is questionable in
6 its proximity due to strong electron-nuclei couplings, making questionable the application of
7 standard optimization methods to explore the non-adiabatic PES. An estimation of the energy
8 barrier for this interconversion at this distance gives a value of the order of $0.2 \text{ kcal}\cdot\text{mol}^{-1}$ (see
9 Supporting Information). All together, *these calculations indicate that the observed biradical*
10 *Ti(III) species are originated by subtle changes of the Ti–O distance in a valence tautomer.*
11 Interestingly, this valence tautomeric equilibrium is reminiscent of the Peierls distortion
12 observed for extended symmetric systems where competition between open and closed shell
13 electronic states is stabilized by small structural distortions.²³

14
15
16
17
18
19
20
21
22
23
24
25
26
27 The parallel analysis of the sulfur-based model **2** revealed a similar but much more intricate
28 situation, since the larger size of sulfur compared to oxygen modifies the bond distances in
29 the rings that modify the shape of the chiral auxiliary. Thus, the biradical character depends
30 on changes of the Ti–S distance as well as two dihedral angles that affect the whole geometry
31 of the chiral auxiliary. Once again, the new electronic character arises from subtle variations
32 of the geometry of the enolate. In this case, the differences of energy between the minima are
33 lower than those observed in **1**.

44 45 **EPR studies on titanium enolates**

46
47
48
49
50 The theoretically predicted low energy triplet electronic state, $\Psi_{\text{os}}^{\text{trip}}$, was experimentally
51 identified by EPR studies of the the Ti(III) biradical species coexistent with titanium(IV)
52 enolate derived from 4-benzyl-5,5-dimethyl-*N*-propanoyl-1,3-oxazolidin-2-one used in our
53 synthetic studies (Scheme 2). The EPR spectrum of this enolate at low temperature (Figure 4)

1
2
3 showed a clear $|\Delta m_s = 1|$ signal with two superimposed bands centered at 3500 G and 3800 G
4
5 and with a remarkable half field $|\Delta m_s = 2|$ fingerprint at ≈ 1580 G, which indicates the
6
7 existence of an electronic triplet state. We assign this signal to the Ti(III) enolate intermediate
8
9 T with open shell structure. These spectroscopic data are in close agreement with the
10
11 computational calculations and all together the results lend a strong support to the coexistence
12
13 of a biradical intermediate and a closed shell titanium complex that can interconvert through a
14
15 low energy transition state.²⁵ This result is in line with previous studies in similar Ti(IV)
16
17 complexes in which the EPR signals have been unambiguously assigned based in the
18
19 observed fine structure and temperature dependence of the spectra.^{12,13}
20
21
22
23
24



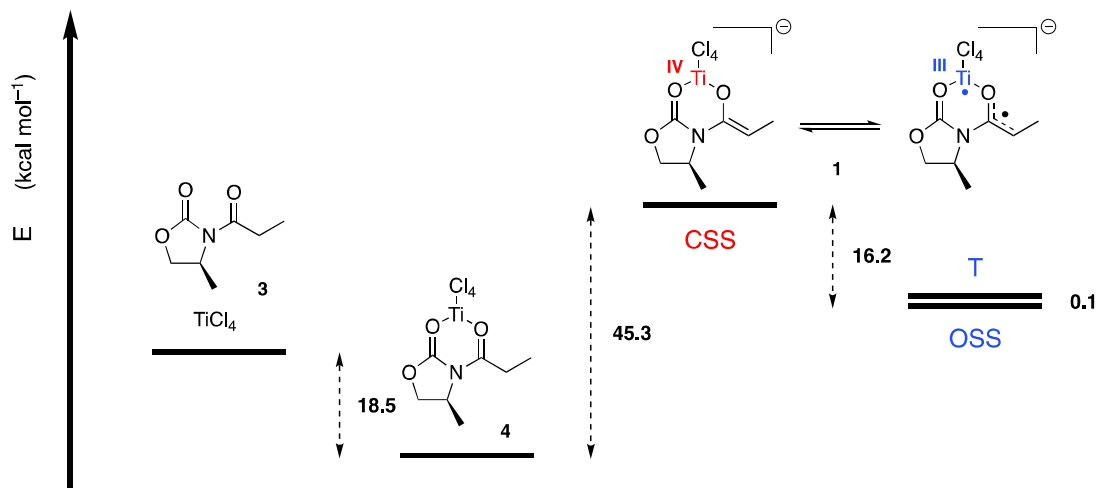
25
26
27
28
29
30
31
32
33
34
35
36
37
38
39
40
41 **Figure 4.** EPR of the Ti(III) biradical species coexistent with the titanium(IV) enolate derived from 4-benzyl-
42 5,5-dimethyl-*N*-propanoyl-1,3-oxazolidin-2-one at 5 K in CH₂Cl₂ solution.²⁵
43
44
45
46
47

48 **The mechanism of the aminoxylation of titanium enolates with TEMPO**

49
50
51
52

53 Having revealed the electronic structure of the titanium(IV) enolates derived from *N*-acyl
54 oxazolidinones, we next assessed the reaction of **1** with a stable radical species such as
55 TEMPO,²⁶ which might be a model for the mechanistic understanding of the titanium-
56
57
58
59
60

mediated aminoxylation of *N*-acyl-4-benzyl-5,5-dimethyl-1,3-oxazolidin-2-ones developed by some of us.²¹



Scheme 3. Reaction profile for the formation of the titanium enolate **1** and its valence tautomerism *in vacuo* using wave-function methods and 6-31G* basis set.

First step: enolization

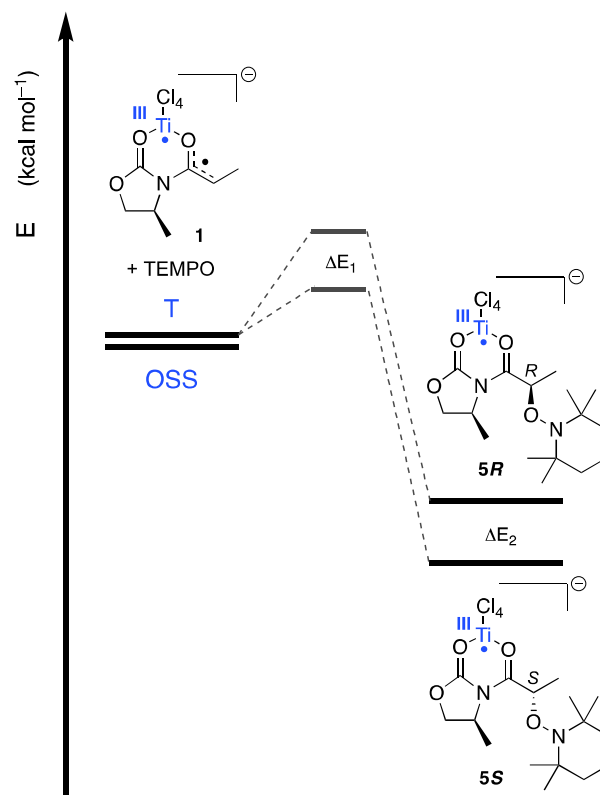
The first step of the sequence was the enolization of the parent *N*-propanoyl oxazolidinone **3** with $\text{TiCl}_4/\text{Et}_3\text{N}$.²⁷ As anticipated, the interaction of **3** with TiCl_4 produced a stable chelated intermediate **4** ($-18.5 \text{ kcal mol}^{-1}$, Scheme 3), which was subsequently deprotonated to give the titanium(IV) enolate **1**. As shown in Scheme 3, the closed shell singlet configuration (CSS) of **1** turned out to be less stable than the open shell configurations, T and OSS, in about 10 kcal mol^{-1} , which highlights the importance of the biradical component to understand both the structure and the reactivity of titanium enolates. The solvent effects on the energy barriers *in vacuo* shown in Scheme 3 are expected to largely reduce the energy cost for the proton extraction step since the species involved change their net charge. Indeed, a model of this reaction in CH_2Cl_2 solution using the conductor-like polarizable continuum model (C-PCM)^{38,39} shows that the energy cost for the proton extraction in the enolization step is largely

1
2
3 reduced and the CSS Ti(IV) species becomes more stable than **4** by ~ 20 kcal mol⁻¹. However,
4
5 the general qualitative shape is maintained, especially in the open shell region of the potential
6
7 energy surface where the open shell structures are further stabilized (see Supporting
8
9 Information for details).
10

11
12
13
14 *Second step: addition of a TEMPO molecule*
15

16 With a firmly based description of the structure of enolate **1** to hand, we next examined the
17
18 second step. This involved the approach of a TEMPO molecule to **1** to form the C–O bond,
19
20 which was the crucial step of the aminoxylation reaction. Our calculations revealed that the
21
22 less sterically hindered π -face of the biradical configuration of the titanium(IV) enolate,
23
24 which could be viewed as a formal titanium(III) radical complex, permitted an easy
25
26 interaction with the TEMPO molecule and the C–O bond could be formed in a low barrier
27
28 transformation that produced the titanium(III) chelate **5** (Scheme 4). If the TEMPO molecule
29
30 approached the enolate from the more sterically hindered π -face the barrier would be 1–2 kcal
31
32 mol⁻¹ larger.²⁸
33
34
35

36 Unfortunately, the transition states of these additions are difficult to localize and characterize
37
38 and the barriers difficult to evaluate due to the size of the molecules and the nature of the
39
40 radical-radical addition that usually shows a small barrier dominated by steric repulsions.
41
42 Thus, the differences of energy of the alternative transition states (ΔE_1), required to predict
43
44 the diastereoselectivity (**5S** versus **5R** in Scheme 4) of the reaction with TEMPO, were
45
46 estimated from the relative stability of the products (ΔE_2) following a thermodynamic
47
48 approach, which assumes that the differences in energy between transition states are
49
50 proportional to those in the resultant products. Such an approach is reasonable since the
51
52 structures of the transition states and the related reactants must be similar because these are
53
54 ~ 25 kcal mol⁻¹ higher in energy than the products.
55
56
57
58
59
60

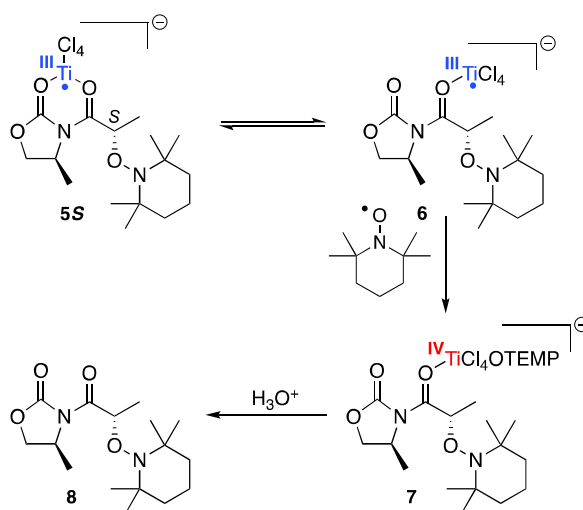


Scheme 4. Reaction profile for the second step at the 6-31G*/UB3LYP level of theory.

Third step: oxidation of titanium(III) chelate 5

Since the experimental development of the aminoxylation reaction had established the need for two equivalents of TEMPO, we next assessed the role of the second molecule of TEMPO. It was clear from the outset that it should be associated with the significant reducing character of the titanium(III) chelate. This was indeed the case, but the mechanistic description of the process turned out to be troublesome. In fact, the oxidation of the titanium(III) involved a multi-equilibrium process in which the hexacoordinated chelate **5S** possessing two weak dative bonds was transformed into a pentacoordinated Ti(III) complex **6**. This was the intermediate that was oxidized by the second TEMPO molecule thereby producing the

1
2
3 titanium(IV) complex **7**, which finally delivered the adduct **8** after the acid work-up (Scheme
4
5). The oxidized complex is 25–30 kcal mol⁻¹ less stable than the Ti(III)-TEMPO anion
6
7 radical adduct plus the additional TEMPO molecule as suggested by preliminary calculations
8
9 using our model *in vacuo*. This energy difference is expected to be further reduced in a polar
10
11 solvent that stabilizes large charged molecular species. Noticeably, the proposed mechanism
12
13 requires much less energy than the direct oxidation of **5S**, which makes necessary to take into
14
15 account the formation of the non-chelated complex **6** and the subsequent ligand exchange.¹³
16
17
18
19
20



39 **Scheme 5.** Third step: oxidation of **5S**.

40
41
42
43
44
45 **Further analysis**

46
47
48
49 Regioselectivity in conjugate enolates

50
51
52 The abovementioned mechanistic model was further applied to account for the
53
54 regioselectivity of the aminoxylation of conjugated enolates. Close inspection of the
55
56 electronic structure of **1** and model conjugated titanium enolates **9** and **10** indicated that the
57
58
59
60

1
2
3 coefficients of the SOMO orbitals at the α , γ , and ϵ positions were comparable, whereas those
4
5 of the β and δ positions were negligible (Figure 5).
6
7
8
9

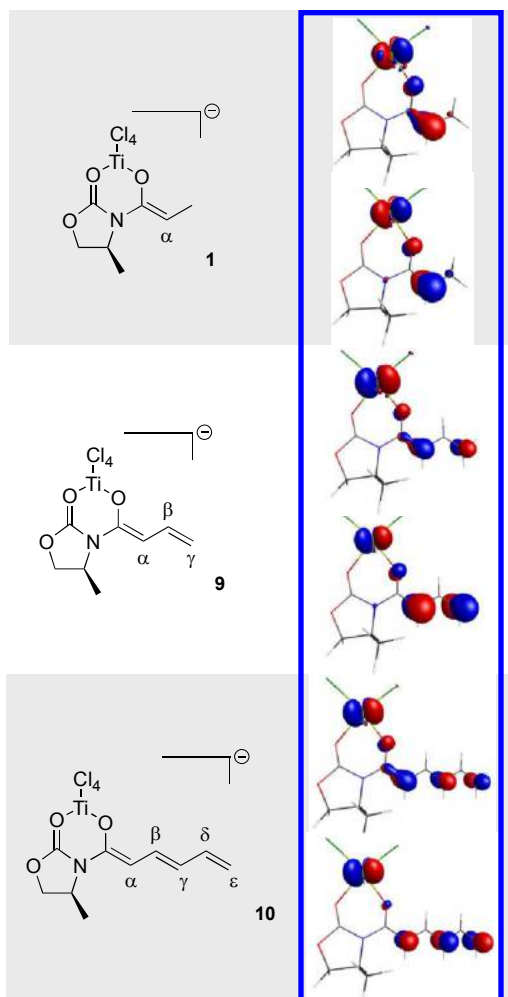
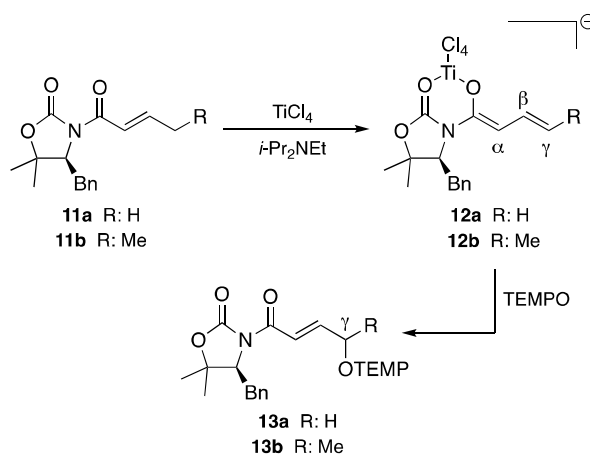


Figure 5. SOMO orbitals of conjugated titanium(IV) enolates taken from monooccupied natural UB3LYP orbitals.

In turn, experimental studies had established that the addition of TEMPO to the titanium(IV) enolates **12a-b** derived from *N*-acyl oxazolidinones **11a-b** shown in Scheme 6 took place exclusively at the γ position;²¹ adducts from the attack to the α or β positions were never observed. All together, these results show that the siteselectivity of conjugated enolates is

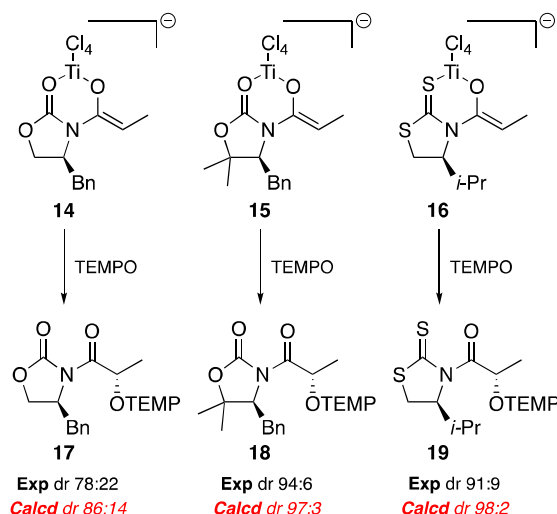
primarily based on orbital topology, but also relies on the poorer accessibility of the α position. Unfortunately, the attack of TEMPO to the γ position of **12b** (R: Me) afforded a 1:1 diastereomeric mixture of adduct **13b**, which indicated that the lack of stereocontrol of the addition to the γ position was due to the large distance from the chiral centre and the ineffective induction by the chiral auxiliary.



Scheme 6. Siteselective aminoxylation reactions of **12**.

Diastereoselectivity

Finally, the diastereoselectivities of the TEMPO-aminoxylation of the titanium(IV) enolates derived from several *N*-propanoyl oxazolidinones and thiazolidinethiones **14–16** represented in Scheme 7 were examined using a simple 6-31G*/UB3LYP approach and the diastereomeric ratios were estimated using the formula $P_S/P_R = \exp(-\Delta E_1/k_B T)$ in which $\Delta E_1 \approx \Delta E_2$ (see Scheme 4).



Scheme 7. Diastereoselective TEMPO-aminoylation of titanium(IV) enolates from *N*-acyl chiral auxiliaries.

We found that the predicted diastereomeric ratios nicely matched the experimental trends. This definitely proves the accuracy of the mechanism we report and the validity of our theoretical analysis. Particularly, these calculations indicated that the excellent diastereoselectivity attained with the titanium(IV) enolate from chiral 4-benzyl-5,5-dimethyl-*N*-propanoyl-1,3-oxazolidin-2-one **15**, much better than that of the parent oxazolidinone **14**, is due to a rigidity of the complex induced by steric repulsion of the geminal methyl groups with the benzyl group that provides a larger exposure of the π -face opposite to the benzyl group. In turn, the distortion produced by the long carbon-sulfur bonds in the thiazolidinethione-derived titanium enolate **16** also facilitates the approach of the electrophile to the opposite face to the isopropyl group and is thus the reason for the high stereocontrol achieved in this case.²⁹

CONCLUSIONS

In summary, quantum chemical calculations have established that the appropriate description of the electronic structure of the titanium(IV) enolates derived from oxazolidinones and thiazolidinethiones includes a *valence tautomerism* equilibrium that involves a closed shell and two open shell configurations. As the energy gap between the closed and the open shell configurations is small, subtle changes to the Ti–O distance makes the OSS configuration the most stable with a thermally accessible triplet state T. This reveals the biradical character of these intermediates which are formally Ti(III) enolates. Such a biradical character has been measured in EPR studies and has been established as the source of radical-like reactivity, which is complementary to the most common nucleophilic profile. In this context, the mechanism of the aminoxylation reaction of titanium(IV) enolates from oxazolidinones with TEMPO has been satisfactorily explained on radical grounds. Importantly, the resulting model accounts for the regio- as well as the diastereoselectivity of such a transformation, which strongly supports the abovementioned calculations. Therefore, both the structure and the reactivity of titanium(IV) enolates, and potentially enolates of other metal, should be examined from this new point of view. Summarizing, the general guideline derived from this study is that titanium(IV) enolates undergo a valence tautomerism equilibrium leading to a coexisting Ti(III) biradical species at normal conditions that should be taken in consideration for a general understanding of their reactivity. Therefore, it should be expected that titanium(IV) enolates can behave either as classical electrophiles or as biradicals depending on the molecule faced by this reagent. One can take advantage of both types of reactivity by choosing an appropriate counterpart and controlling the reaction conditions.

EXPERIMENTAL SECTION

Theoretical methods

All our calculations on the valence tautomerism of titanium(IV) enolates and their reaction with TEMPO were carried out *in vacuo* employing the standard 6-31G* basis set and GAMESS 2012 package.^{30,31} The all electron basis set corresponds to that reported by Pople and collaborators: [4s/2s] for H and [10s4p1d/3s2p1d] for C, N, and O;³² [16s10p1d/4s3p1d] for Cl and S,³³ and [22s16p4d1f/5s4p2d1f] for Ti.³⁴

Regarding the methods used to describe the electronic structure of the intermediates, for the enolization step and valence tautomerism process we have used wave function methods (Hartree-Fock (HF) for closed shell structures and Complete Active Space Self Consistent Field (CASSCF) methods for the multireferential states (CSS, OSS and T) whereas UB3LYP method has been used to describe the intermediate structures involved in the first and second TEMPO additions to understand their regio- and stereoselectivity.

In our studies on the first step of the aminoxylation reaction the structure of the starting oxazolidinone **3** and the TiCl₄-complex **4** were evaluated at RHF level, whereas the structures involved in the valence tautomerism of the titanium enolate were calculated at CASSCF(8,7) level due to the multireference nature of the electronic states involved. The selection of the CAS(*m*, *n*) was performed using the standard method³⁵ based on occupation numbers of the UMP2 natural orbitals for the **T** state (those having $1.98 < n < 0.2$) that provided a consistent orbital space for the **T**, **OSS** and **CSS** electronic states beyond the minimum CAS (4,4) space. However, for compound **2** it was not possible to define a consistent orbital space beyond CAS(4,4). Nevertheless, the description of these electronic states at CASSCF(4,4) provide molecular structures and energy profile similar to the one shown in Scheme 3.

1
2
3 Calculations on the chiral TEMPO adducts to obtain ΔE_2 were performed using the UB3LYP
4
5 approach as implemented in the GAMESS package. This DFT approach allows us to study
6
7 much more complex systems than the method used in former studies. However, the
8
9 application of DFT methods based on a single Kohn-Sham determinant to represent the
10
11 electronic states of open shell systems is questionable,^{36,37} especially for multireference states
12
13 such as **CSS** or **OSS**. Nevertheless, a close inspection of the wave functions of the **T** state and
14
15 the doublet species such TEMPO or the TEMPO adducts can be approximately described by a
16
17 single determinant with well localized open shell orbitals and, hence, this kind of
18
19 approximation is justified. The fact that the relevant energy differences in the reaction profiles
20
21 investigated are due to conformational differences of the organic part the B3LYP functional
22
23 provides, in principle, a standard, simple and balanced description for a qualitative
24
25 rationalization of the processes.
26
27
28

29
30 Solvent effects on the enolization step of the proposed mechanism have been analyzed by
31
32 means of the conductor-like polarizable continuum model (C-PCM)^{38,39} implemented in the
33
34 GAMESS code,^{30,31} using CH_2Cl_2 as a solvent. In all cases, zero point energy corrections
35
36 have been considered.
37
38
39

40 41 42 43 44 45 46 **ASSOCIATED CONTENT**

47 48 49 50 **Supporting Information**

51
52
53 The Supporting Information is available free of charge on the ACS Publications website at
54
55 <http://pubs.acs.org>.
56
57
58
59
60

1
2
3 Supplementary Tables S1–S4 contain Cartesian coordinates of the optimized molecular
4
5 structures described in the text, Supplementary Figure S1 describes some structure details of
6
7 the species involved in the valence tautomerism of **1** and **2**, Supplementary Figure S2
8
9 describes the relevant CASSCF(4,4) natural orbitals of the electronic configurations of **2** and
10
11 the final section Additional calculations describe the results of the calculations performed to
12
13 investigate the solvent effects on the enolization process of compound **1** and an approximate
14
15 structure of the transition structure between CSS and OSS/T in the IC region of the PES.
16
17
18
19
20
21
22

23 AUTHOR INFORMATION

26 Corresponding author

27
28 E-mail: i.moreira@ub.edu

30 Notes

31
32 The authors declare no competing financial interests.
33
34
35
36
37
38
39

40 ACKNOWLEDGEMENTS

41
42
43 Financial support from the Spanish Ministerio de Economía y Competitividad and Fondos
44
45 Feder (Grant Nos. CTQ2012-31034, CTQ2015-65759, and CTQ2016-76423-P) and the
46
47 Generalitat de Catalunya (2009 SGR825 and 2014 SGR586) as well as a predoctoral
48
49 studentship to A. G.-P. (APIF, Universitat de Barcelona) are acknowledged.
50
51
52
53
54
55

56 REFERENCES

57
58
59
60

- 1
2
3 (1) Zabicky, J. *The Chemistry of Metal Enolates (Patai's Chemistry of Functional*
4 *Groups)* (Rappoport, Z. Ed.); Wiley-VCH: Chichester, 2009.
5
6
7 (2) Meikelburger, H. B.; Wilcox, C. S. In *Comprehensive Organic Synthesis (2nd Edition)*,
8 *Vol. 2* (Knochel, P.; Molander, G. A. Eds.); Elsevier, Amsterdam: 2014, pp. 243–272.
9
10
11 (3) Carreira, E. M.; Kvaerno, L. *Classics in Stereoselective Synthesis*; Wiley-VCH:
12 Weinheim, 2009.
13
14
15 (4) Stoltz, B. M.; Bennett, N. B.; Duquette, D. C; Goldberg, A. F. G.; Liu, Y.; Loewinger,
16 M. M.; Reeves, C. M. In *Comprehensive Organic Synthesis (2nd Edition)*, *Vol. 3* (Knochel, P.
17 G. Molander, A. Eds.); Elsevier: Amsterdam, 2014, pp. 1–55.
18
19
20 (5) *Modern Methods in Stereoselective Aldol Reactions*, (R. Mahrwald Ed.); Wiley-VCH:
21 Weinheim, 2013.
22
23
24 (6) For a comprehensive and insightful analysis on the structure and reactivity of lithium
25 enolates, see: (a) Renny, J. S.; Tomasevich, L. L.; Tallmadge, E. H.; Collum, D. B. *Angew.*
26 *Chem. Int. Ed.*, **2013**, *52*, 11998–12013. (b) E. H. Tallmadge, D. B. Collum, *J. Am. Chem.*
27 *Soc.* **2015**, *137*, 13087–13095.
28
29
30 (7) For a representative example, see Yu, K.; Lu, P.; Jackson, J. J.; Nguyen, T.-A. D.;
31 Alvarado, J.; Stivala, C. E.; Ma, Y.; Mack, K. A.; Hayton, T. W.; Collum, D. B.; Zakarian, A.
32 *J. Am. Chem. Soc.* **2017**, *139*, 527–533.
33
34
35 (8) Ligands are said to be *innocent* when they allow oxidation states of the central atoms
36 to be well defined and permanent. See: Jørgensen, C. K. *Coordin. Chem. Rev.*, **1966**, *1*, 164–
37 178.
38
39
40 (9) (a) de Bruin, B. *Eur. J. Inorg. Chem.*, **2012**, 340–342. (b) Luca, O. R.; Crabtree, R. H.
41 *Chem. Soc. Rev.*, **2013**, *42*, 1440–1459.
42
43
44 (10) For the role of *non-innocent* ligands in catalysis, see: (a) Chirik, P. J.; Wieghardt, K.
45 *Science*, **2010**, *327*, 794–795. (b) Dzik, W. I.; van der Vlugt, J. I.; Reek, J. N. H.; de Bruin, B.
46
47
48
49
50
51
52
53
54
55
56
57
58
59
60

1
2
3 *Angew. Chem. Int. Ed.*, **2011**, *50*, 3356–3358. (c) Lyaskovskyy, V.; de Bruin, B. *ACS Catal.*,
4
5 **2012**, *2*, 270–279.

6
7 (11) (a) Evangelio, E.; Ruiz-Molina, D. *Eur. J. Inorg. Chem.*, **2005**, 2957–2971. (b)
8
9 Tezgerevska, T.; Alley, K. G.; Boskovic, C. *Coordin. Chem. Rev.*, **2014**, *268*, 23–40.

10
11 (12) Moreira, I de P. R.; Bofill, J. M.; Anglada, J. M.; Solsona, J. G.; Nebot, J.; Romea, P.;
12
13 Urpí, F. *J. Am. Chem. Soc.*, **2008**, *130*, 3242–3243.

14
15 (13) Heras, C.; Ramos-Tomillero, I.; Caballero, M.; Paradís-Bas, M.; Nicolás, E.; Albericio,
16
17 F.; Moreira, I. de P. R.; Bofill, J. M. *Eur. J. Org. Chem.*, **2015**, 2111–2118.

18
19 (14) For a recent overview on the titanium(IV) enolate chemistry, see: Ciez, D.; Palasz, A.;
20
21 Trzewik, B. *Eur. J. Org. Chem.*, **2016**, 1476–1493.

22
23 (15) (a) Kise, N.; Ueda, T.; Kumada, K.; Terao, Y.; Ueda, N. *J. Org. Chem.*, **2000**, *65*,
24
25 464–468. (b) Nguyen, P. Q.; Schäfer, H. J. *Org. Lett.*, **2001**, *3*, 2993–2995.

26
27 (16) Csáký, A. G.; Plumet, J. *Chem. Soc. Rev.* **2001**, *30*, 313–320.

28
29 (17) Richter, J. M.; Whitefield, B. W.; Maimone, T. J.; Lin, D. W.; Castroviejo, M. P.;
30
31 Baran, P. S. *J. Am. Chem. Soc.*, **2007**, *129*, 12857–12869.

32
33 (18) (a) Beaumont, S.; Ilardi, E. A.; Monroe, L. R.; Zakarian, A. *J. Am. Chem. Soc.*, **2010**,
34
35 *132*, 1482–1483. (b) Herrmann, A. T.; Smith, L. L.; Zakarian, A. *J. Am. Chem. Soc.*, **2012**,
36
37 *134*, 6976–6979. (c) Gu, Z.; Herrmann, A. T.; Zakarian, A. *Angew. Chem. Int. Ed.*, **2011**, *50*,
38
39 7136–7139.

40
41 (19) For an overview, see Amatov, T.; Jahn, U. *Angew. Chem. Int. Ed.*, **2011**, *50*, 4542–
42
43 4544.

44
45 (20) Mabe, P. J.; Zakarian, A. *Org. Lett.*, **2014**, *16*, 516–519.

46
47 (21) Gómez-Palomino, A.; Pellicena, M.; Romo, J. M.; Solà, R.; Romea, P.; Urpí, F.; Font-
48
49 Bardía, M. *Chem. Eur. J.*, **2014**, *20*, 10153–10159.

1
2
3 (22) In fact, enolates **1** and **2** are *ate complexes*. The putative titanium(IV) enolates
4 should contain three chlorine atoms bound to the titanium metal without a net charge.
5
6 However, such species have been calculated to be much less stable than the aforementioned
7
8
9
10 *ate complexes*.

11 (23) Salem, L. In *The Molecular Orbital Theory of Conjugated Systems*; W. A. Benjamin:
12 New York, 1966, pp. 495–505.
13

14 (24) The potential energy surfaces of different spin symmetry can intersect in a hyperline
15
16 called *seam*. The two potential energy surfaces, each one corresponding to singlet states, lead
17
18 to a conical intersection or a weakly avoided crossing depending on the nature of the
19
20 electronic states involved. See Schlegel H. B. *Modern Electronic Structure Theory, Part I*
21
22 (Yarkony, D. R., Ed.); World Scientific: Singapore, 1995.
23
24

25 (25) The EPR spectra of the titanium enolates (X-band, □□□□ 9.414185 GHz) have been
26
27 recorded at 5 K in CH₂Cl₂ solution after reacting the corresponding ketone with TiCl₄ and
28
29 triethylamine under inert atmosphere. Standard blank ground line correction has been applied
30
31 and do not show any signal in the explored regions. Consequently these signals are
32
33 unambiguously assigned to the Ti(III) enolate intermediate T with open shell structure.
34
35 Similar studies were carried out on sulfur-based analogs. Unfortunately, these compounds
36
37 produce EPR signals of much lower intensity even at low temperature. This observation can
38
39 be expected since the OSS and T biradical states of these derivatives are predicted to be closer
40
41 in energy to the CSS state (5.8 kcal mol⁻¹).
42
43
44
45

46 (26) For the use of TEMPO and other nitroxides in synthesis, see: (a) Vogler, T.; Studer, A.
47
48 *Synthesis*, **2008**, 1979–1993. (b) Tebben, L.; Studer, A. *Angew. Chem. Int. Ed.*, **2011**, *50*,
49
50 5034–5068.
51
52

53 (27) Evans, D. A.; Urpí, F.; Somers, T. C.; Clark, J. S.; Bilodeau, M. T. *J. Am. Chem. Soc.*,
54
55 **1990**, *112*, 8215–8216.
56
57
58
59
60

- 1
2
3 (28) The triplet state of the enolate has been used to calculate the approach to the TEMPO
4 molecule, which gives the adduct in the doublet electronic state.
5
6
7 (29) For the influence of chiral auxiliaries on stereoselective reactions from titanium
8 enolates, see Baiget, J.; Cosp, A.; Gálvez, E.; Gómez-Pinal, L.; Romea, P.; Urpí, F.
9
10 *Tetrahedron*, **2008**, *64*, 5637–5644.
11
12 (30) Schmidt, M. W.; Baldrige, K. K.; Boatz, J. A.; Elbert, S. T.; Gordon, M. S.; Jensen, J.
13 H.; Koseki, S.; Matsunaga, N.; Nguyen, K. A.; Su, S.; Windus, T. L.; Dupuis, M.;
14 Montgomery, J. A., Jr. *J. Comput. Chem.*, **1993**, *14*, 1347–1363.
15
16 (31) Gordon, M. S.; Schmidt, M. W. In *Theory and Applications of Computational*
17 *Chemistry, the first forty years* (Dykstra, C. E.; Frenking, G.; Kim, K. S.; Scuseria, G. E.,
18 Eds), Chapter 41, pp. 1167–1189. Elsevier: Amsterdam, 2005.
19
20 (32) Hariharan, P. C.; Pople, J. A. *Theoret. Chimica Acta*, **1973**, *28*, 213–222.
21
22 (33) Francl, M. M.; Petro, W. J.; Hehre, W. J.; Binkley, J. S.; Gordon, M. S.; DeFrees, D.
23 J.; Pople, J. A. *J. Chem. Phys.*, **1982**, *77*, 3654–3665.
24
25 (34) Rassolov, V.; Pople, J. A.; Ratner, M.; Windus, T. L. *J. Chem. Phys.*, **1998**, *109*,
26 1223–1229.
27
28 (35) Bofill, J. M.; Pulay, P. *J. Chem. Phys.*, **1989**, *90*, 3637–3646.
29
30 (36) Caballero, M.; Moreira, I. de P. R.; Bofill, J. M. *J. Chem. Phys.*, **2013**, *138*, 174107.
31 Mol. Phys. *112*, 809 (2013) and *J. Chem. Phys.* *138*, 174107 (2013)
32
33 (37) Caballero, M.; Moreira, I. de P. R.; Bofill, J. M. *Mol. Phys.*, **2013**, *112*, 809–817.
34
35 (38) Barone, V.; Cossi, M. *J. Phys. Chem. A*, **1998**, *102*, 1995–2001.
36
37 (39) Cossi, M.; Rega, N.; Scalmani, G.; Barone, V. *J. Comput. Chem.* **2003**, *24*, 669–681.
38
39
40
41
42
43
44
45
46
47
48
49
50
51
52
53
54
55
56
57
58
59
60